ISSN 2347 - 3983
Volume 12. No.3, March 2024
International Journal of Emerging Trends in Engineering Research
Available Online at http://www.warse.org/IJETER/static/pdf/file/ijeter011232024.pdf
https://doi.org/10.30534/ijeter/2024/011232024

New Speed Control Scheme for a Three-Phase Induction Machines - (3~IM) Based on Sine Duty Cycle Modulation (SDCM)

Nykie Edima Ze[1], Arnaud Biyobo Obono[2], Paul Etouké Owoundi[3], Gabriel Roméo Tobajio Haoudou[4], Léandre Nneme Nneme[5], Jean Mbihi[6]

[1,2,3,4,5,6] Research Laboratory of Computer Science Engineering and Automation
Doctorate Training Unit for Engineering Sciences
Doctorate School for Pure and Applied Sciences
ENSET, University of Douala, Cameroon
edimazenykie@gmail.com

Received Date: January 25, 2024 Accepted Date: February 24, 2024 Published Date : March 07, 2024

ABSTRACT

This paper proposes a new control scheme for three-phase induction machines based on the sinusoidal duty cycle modulation control strategy combined with *V/f* control. This technique allows efficient open-loop control of inverter switches. The proposed diagram shows the main characteristics: $\alpha_1 = 0.1$, $f_0 = 50Hz$, $f_{base} = 21.44KHz$, $u_{ref} = [2V, 12V]$. In addition, it guarantees optimum operation of the inverter with the torque and speed parameters of the three-phase induction machine complying with current requirements: $C_r = 10\,Nm$ $I_{S\max} = 6{,}5A/50Hz/$ THD=1,2%

Key words: Matlab/Simulink, Modeling, Open loop, SDCM**,** Three-phase induction machines.

1. INTRODUCTION

Three-phase induction machines (TIMs) are widely used in industrial and domestic applications, thanks to their reliability, low cost and easy maintenance. However, controlling the speed of these machines is a complex problem, as it involves modifying the voltage and frequency of the network that supplies them. Various techniques have been proposed [1-7] to achieve this control, of which scalar *V/f* control is one of the simplest and most effective. This technique consists of supplying the MIT with an inverter controlled by pulse width modulation (PWM), which generates a variable voltage and frequency as a function of the speed setpoint.

In this work, we propose a new speed control scheme for a three-phase asynchronous machine (ASM), based on sinusoidal duty cycle modulation (SDCM). This technique allows efficient control of the inverter switches supplying the ASM. SRCM has several advantages [8-20] such as hardware simplicity, low implementation cost, attractive modulation properties, self-modulation and simple design of good quality inverters. MRC was initially introduced for industrial instrumentation applications, such as analogue-to-digital conversion (ADC) [21], digital-to-analogue conversion (DAC) [22] and analogue signal transmission [23]. However, its application to the control of electrical machines is still relatively unexplored.

Our contribution in this work is to study the feasibility of open-loop speed control of a ASM using the SDCM technique, combined with *V/f* control. This study will therefore make it possible to control the speed of a ASM using a very simple, effective and less costly structure, to reduce voltage drops and energy losses and to increase the service life of the machine and associated electrical equipment.

The plan of this article is as follows: Section 2 details the various analysis tools and methods used to investigate the new control architecture of a three-phase induction machine. Section 3 provides an exhaustive presentation of the results obtained through virtual simulations carried out in the Matlab/Simulink environment, together with an in-depth analysis. Finally, Section 4 brings this work to a close with a substantial conclusion, while outlining some future prospects for research in this area.

2. TOOLS AND METHODS

2.1. General synoptic of the control scheme by SDCM

The general synoptic of the new three-phase induction machine control scheme is shown in Figure 1 above. It consists of a three-phase AC source, an AC/DC converter, an LC filter, a DC/AC converter, an ASM, a driven load and the SDCM control block associated with *V/f* control. In the rest of the work, the rectifier and filter will not be studied $E_f = 500V$.

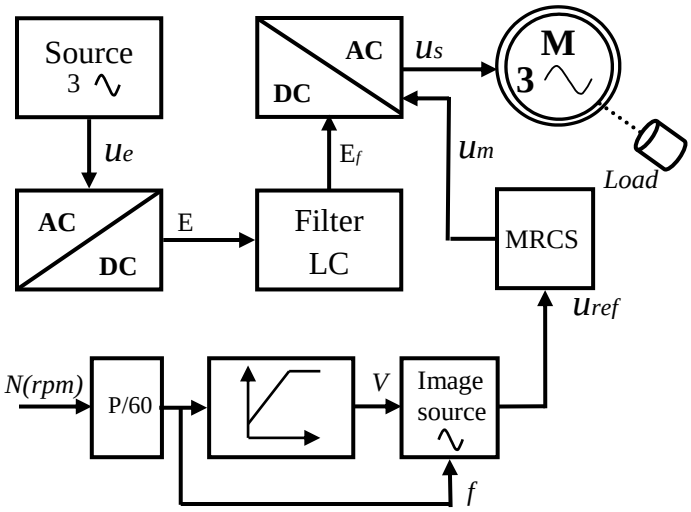

Figure 1: General synoptic

2.2. Modelling duty cycle modulator

The duty cycle modulator represented in Figure 2 by its Simulink model is a negative resistance-controlled oscillator whose operating principle is based on charging and discharging the capacitor at a time constant of [8]. The voltage obtained is compared with a sinusoidal voltage (modulating signal) in order to obtain the control signal needed to drive the inverter switches.

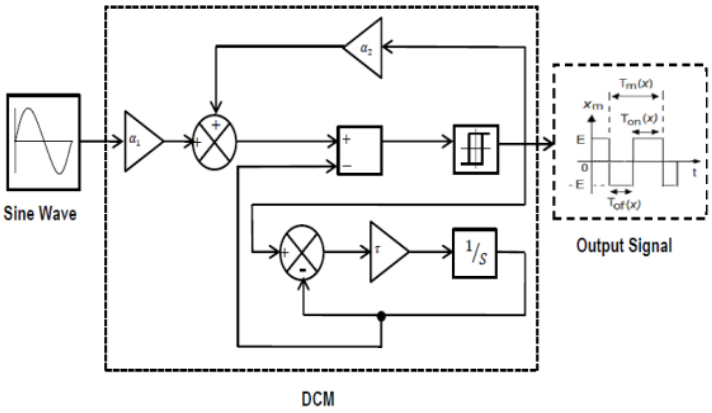

Figure 2 : Simulink SDCM

This Simulink model of the modulator has been presented at length and in detail in previous works. However, on the basis of research published in the literature, we recall that an MRC signal denoted Xm(t) and its characteristic quantities denoted Rm(x(t)) = duty cycle, Toff(x(t)) = positive pulse duration, Tm(x(t)) = modulation period, are respectively described by relations (1) to (4), available in [8-11].

$$R_m\left(x(t)\right)=\frac{T_{on}\left(x(t)\right)}{T_m\left(x(t)\right)} \qquad (1)$$

$$T_{on}\left(x(t)\right)=\tau\ln\left(\frac{(1-\alpha)x-(1+\alpha)E}{(1-\alpha)x+(\alpha-1)E}\right),\ \text{avec}\ p_m=\frac{\dfrac{\alpha_1\alpha_2}{E(1-\alpha_1^2)}}{\log\left(\dfrac{1+\alpha_1}{1-\alpha_1}\right)} \qquad (2)$$

$$T_m\left(x(t)\right)=\tau\ln\left(\frac{\left((1-\alpha)x\right)^2+\left((1+\alpha)E\right)^2}{\left((1-\alpha)x\right)^2-\left((\alpha-1)E\right)^2}\right) \qquad (3)$$

The exact analytical expression of the modulation duty cycle Rm(x(t)), originally established in [6], is highly non-linear in x. For this reason, it has been shown that there is an excellent linear approximation of from the point of view of accuracy and modulating range by a 1st order Taylor expansion. Relation (4) corresponds to the linearised model of defined in [12- 24].

$$R_m\left(x(t)\right)=p_m x(t)+\frac{1}{2},\ \ avec\ \ p_m=\frac{\dfrac{\alpha_1\alpha_2}{E(1-\alpha_1^2)}}{\log\left(\dfrac{1+\alpha_1}{1-\alpha_1}\right)} \qquad (4)$$

2.3. Modelling three-phase inverter

Switches S_1 and S_1', S_2 and S_2', S_3 and S_3' in Figure 3 are complementary two by two, whatever the control law to be adopted, it is possible to establish general relationships which we will use for MRCS control; whatever the currents, the switches impose the voltages between the output terminals A, B, C and the (fictitious) mid-point 'O' of the voltage source. This operation is described by relations (5) to (6) defined in [25- 26].

$$R_m\left(x(t)\right)=p_m x(t)+\frac{1}{2},\ \ avec\ \ p_m=\frac{\dfrac{\alpha_1\alpha_2}{E(1-\alpha_1^2)}}{\log\left(\dfrac{1+\alpha_1}{1-\alpha_1}\right)}$$

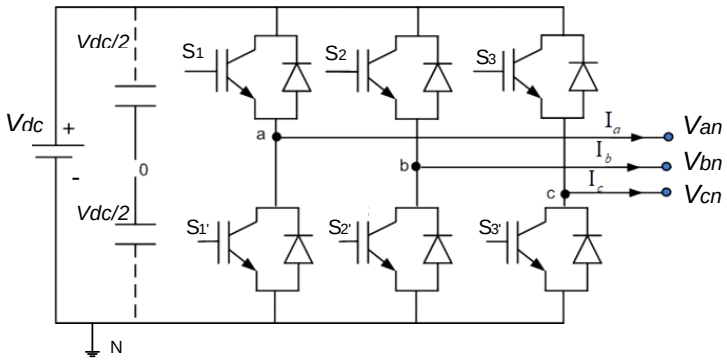

Figure 3: Block diagram of 3~ inverter

$$\begin{cases} V_A - V_O = V_{DC}/2 & S_1 \text{ close} \\ V_B - V_O = V_{DC}/2 & S_2 \text{ close} \\ V_C - V_O = V_{DC}/2 & S_3 \text{ close} \end{cases} \quad (5)$$

$$\begin{cases} V_A - V_O = -V_{DC}/2 & S_1 \text{ open} \\ V_B - V_O = -V_{DC}/2 & S_2 \text{ open} \\ V_C - V_O = -V_{DC}/2 & S_3 \text{ open} \end{cases} \quad (6)$$

Assuming that the receiver is balanced, we can switch from the composite voltages to the simple voltages VA, VB, VC at the output of the inverter. The family of characteristic equations is thus given to systems (7) by

$$: \begin{cases} V_A = \frac{1}{3}\left[2(V_A - V_O) - (V_B - V_O) - (V_C - V_O)\right] \\ V_B = \frac{1}{3}\left[-(V_A - V_O) + 2(V_B - V_O) - (V_C - V_O)\right] \\ V_C = \frac{1}{3}\left[-(V_A - V_O) - (V_B - V_O) + 2(V_C - V_O)\right] \end{cases} \quad (7)$$

Let V_{AO}, V_{BO} and V_{CO} be the inverter input voltages (DC values) and V_A, V_B and V_C the inverter output voltages (AC values). The voltage inverter can be modelled by a DC-AC matrix [T] given by equation (8) below:

$$T = \frac{1}{3}\begin{bmatrix} 2 & -1 & -1 \\ -1 & 2 & -1 \\ -1 & -1 & 2 \end{bmatrix} \quad \text{With} \quad V_{AC} = T.V_{DC} \quad \begin{cases} V_{AC} = V_A, V_B, V_C \\ V_{DC} = V_{ao}, V_{bo}, V_{co} \end{cases} \quad (8)$$

2.4. Modelling the three-phase asynchronous machine

Modelling a three-phase asynchronous machine involves establishing the relationships between the electrical, magnetic and mechanical quantities that characterise its operation. These relationships are generally non-linear and depend on the reference frame chosen to express the variables. For our study, we have opted for a reference frame linked to the rotating field because it is better suited to setting the parameters of the three-phase asynchronous machine. Taking into account the simplifying assumptions [1], [5-7] the mathematical model of the three-axis squirrel-cage induction motor for our case is transformed into a two-axis model (dq) using the PARK transformation. Figure 4 below shows the simplified model of this motor in the dq reference frame. The zero-sequence component is not shown.

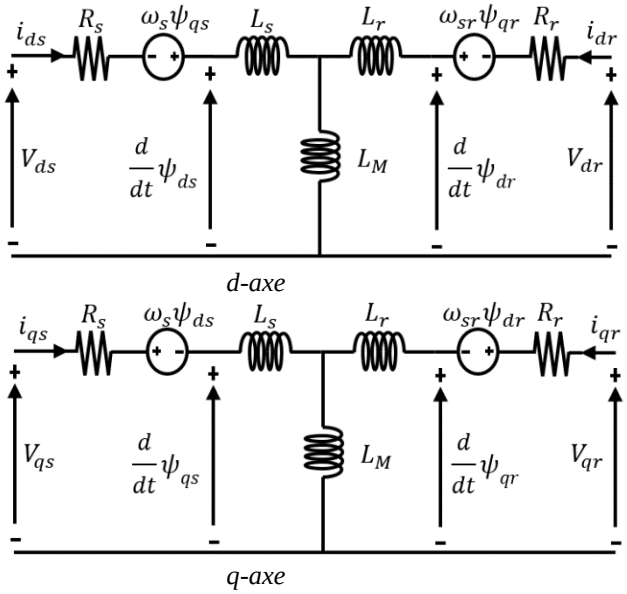

Figure 4: dq equivalent circuits of the three-phase asynchronous motor

The equations below describe the mathematical model of the three-phase asynchronous motor in the park frame of reference. Equation group (9) presents the electrical equations of the machine; equation group (10) presents the magnetic equations and equation group (11) presents the mechanical equations.

$$\begin{cases} V_{ds} = R_s I_{ds} + \frac{d\psi_{ds}}{dt} - \omega_s \psi_{qs} \\ V_{qs} = R_s I_{qs} + \frac{d\psi_{qs}}{dt} + \omega_s \psi_{ds} \\ 0 = R_r I_{qr} + \frac{d\psi_{qr}}{dt} + (\omega_s - \omega_r)\psi_{dr} \\ 0 = R_r I_{dr} + \frac{d\psi_{dr}}{dt} - (\omega_s - \omega_r)\psi_{qr} \end{cases} \quad (9)$$

$$\begin{cases} \psi_{ds} = L_s I_{ds} + L_M I_{dr} \\ \psi_{qs} = L_s I_{qs} + L_M I_{qr} \\ \psi_{dr} = L_r I_{dr} + L_M I_{ds} \\ \psi_{qr} = L_r I_{qr} + L_M I_{qs} \end{cases} \quad (10)$$

$$\begin{cases} C_{em} = p\frac{L_M}{L_r}\left(\psi_{dr} I_{qs} - \psi_{qr} I_{ds}\right) \\ J\frac{d\Omega_r}{dt} = C_{em} - C_r - f\Omega_r \end{cases} \quad (11)$$

3. RESULTS AND DISCUSSIONS

3.1. Virtual Simulation Platform and Structure

Matlab's Simulink environment is the platform used to carry out the virtual simulations on the new scheme presented in this work.

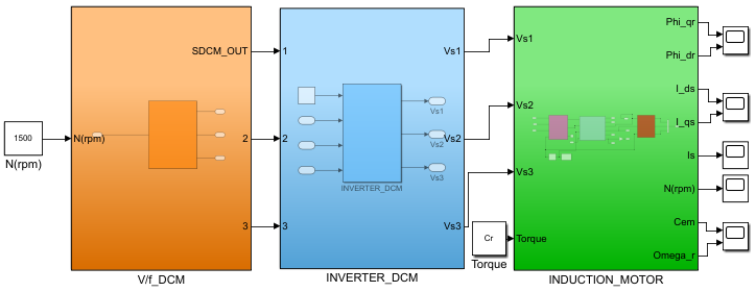

Figure 5: Simulink structure of the 3~ ASM by SDCM control system

The simulation platform shown in Figure 5 above is subdivided into three main blocks: block1 *V/f_* SDCM receives the speed setpoint and generates the control setpoints for the switches of the three-phase inverter in block2 SDCM inverter while keeping the *V/f* ratio constant. The block3 three-phase induction motor is supplied with a high-frequency modulated three-phase voltage. At the output of block3, the main motor parameters are observed.

3.1.1 Simulation parameters

The simulation assumptions and parameters for ***3*~ ASM** presented in Table 1 below are taken from the literature [2].

Table 1 : Simulation parameters

Bloc	Name	Symbol	Valor
V/f_MRCS	SDCM Parameters	α_1	*0.1*
	Frequency u_{ref}	f_0	*50Hz*
	Maximum input voltage	$U_{ref\,\max}$	$[2V, 12V]$
	SDCM base frequency	f_{base}	*21.44Khz*
SDCM Inverter	DC bus voltage	E_f	500*V*
MAS *3*~	Numbers of pole pairs	*p*	*2*
	Rotor resistance per phase	*Rr*	*3,805*Ω
	Stator resistance per phase	*Rs*	*4,85* Ω
	stator inductance	*Ls*	*0,274 H*
	rotor inductance	*Lr*	*0,274 H*
	Mutual cyclic stator-rotor inductance	L_M	*0,258 H*
	Moment of inertia of the rotating part	*J*	*0,031 Kg.m²*
	Coefficient of friction	f_r	*0,001136 Nm/rad/s*
	Rated power	P_n	*1,5 KW*
Load	Torque resistance	C_R	*10Nm*

3.2. Results of simulations and discussions

3.2.1. 3~ ASM idle operation

3.2.1.1. Rotational Speed

Figure 6 below shows the evolution of the motor speed as a function of time for a perfectly sinusoidal supply. After the 0.25s transient phase, the speed has almost reached the reference value of 1500 rpm.

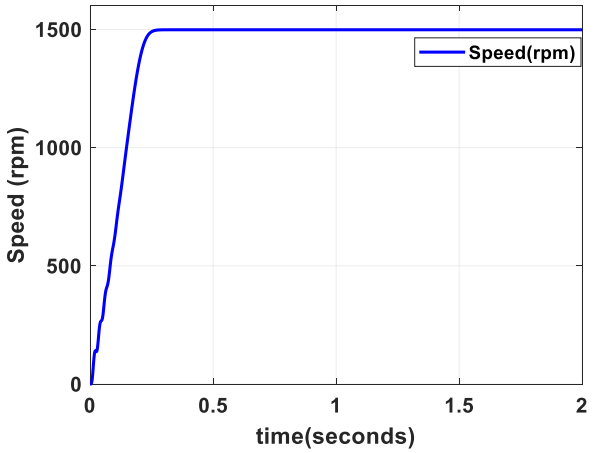

Figure 6: Machine no-load speed characteristic

3.2.1.2. Motor Torque

In the case of an ideal sinusoidal supply, Figure 7 shows the torque during a no-load phase lasting approximately 2 seconds. This shows an oscillating transient regime, reaching its maximum at 44 N.m. In steady state, it stabilises at around 0.2 N.m, providing effective compensation for friction and ventilation losses just after 0.25 seconds.

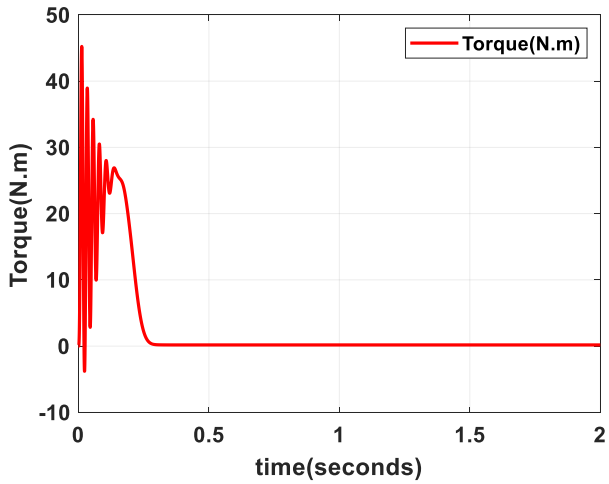

Figure 7: Machine torque characteristic

3.2.1.3. Stator Current

The no-load stator currents, at a perfectly sinusoidal voltage, are balanced sinusoidal alternating currents, as shown in Figure 8. In steady state, they have an amplitude of approximately 3.76 A and a frequency of 50 Hz. On start-up, the current increases to around 24.3 A, with a sinusoidal transient lasting around 0.25 s.

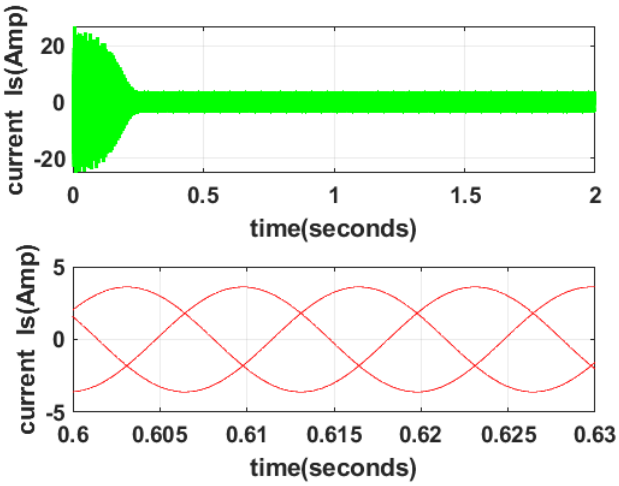

Figure 8: Stator current profiles

3.2.1.4. Stator magnetic flux

The stator no-load magnetic fluxes of the *3*~ ASM in the d and q marks are also shown in Figure 9. These sinusoidal oscillating fluxes are those expected.

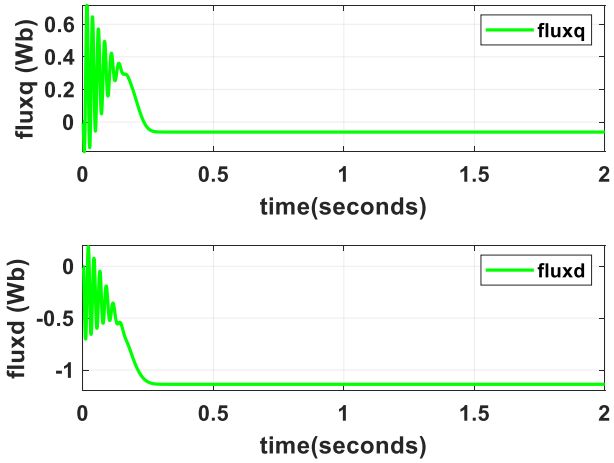

Figure 9: Flux patterns in the dq benchmarks

3.2.2. Load operation of 3~ASM SDCM_V/f (Cr= 10Nm)

3.2.2.1. Rotational Speed

Figure 10 shows the evolution of the speed of rotation under the effect of a mechanical load. At time t=1s, a mechanical load generating a resistive torque of 10 Nm is applied to the rotor, resulting in a reduction in speed from 1500 rpm to around 1300 rpm. This slight decrease in speed reflects additional slip. Open-loop control of the ASM is orchestrated by the SDCM, in conjunction with *V/f* control.

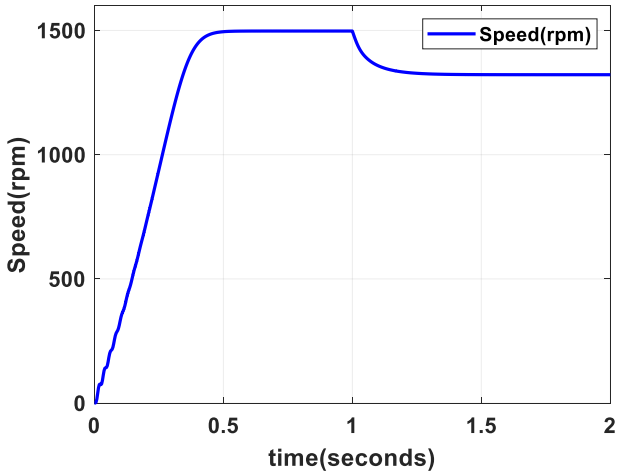

Figure 10: Load speed characteristic of 3~ ASM SDCM_V/f

3.2.2.2. Motor Torque

The time characteristic of the motor torque in Figure 11 below also shows, after a transient phase followed by no-load operation between 0 and 1s, a changeover at t=1s to reach the value of the resistive torque imposed by the load.

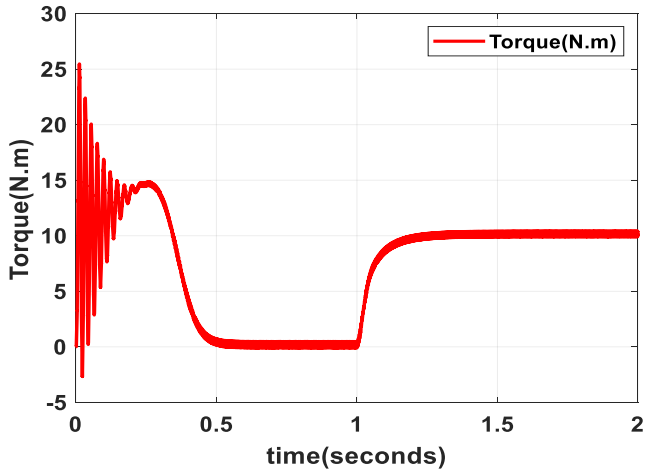

Figure 11: Load torque characteristics of 3~ASM SDCM_V/f

3.2.2.3. Stator Current

The stator currents on load are also balanced sinusoidal alternating currents. After reaching a no-load amplitude of approximately 3A and a frequency of 50 Hz, each abruptly switches to an amplitude of 6.5A at time t=1s.Closer observation of these stator currents in Figure 12 between 1.5s and 1.53s reveals the shape of the signal over this time interval.

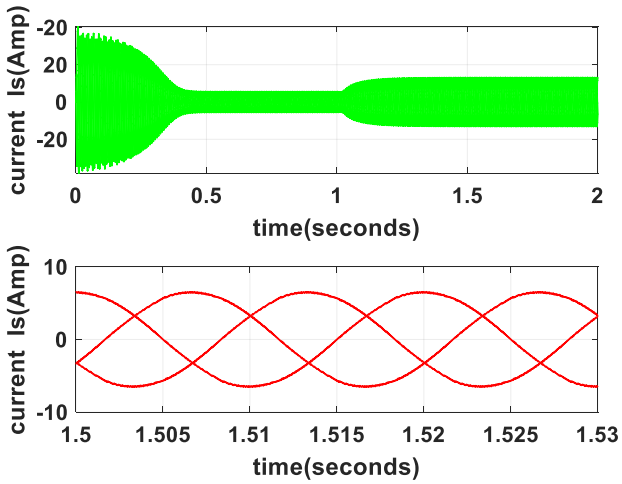

Figure 12: 3~ ASM SDCM_V/f stator current on load

3.2.2.4. Stator magnetic flux

The stator magnetic fluxes for a 10Nm load on the shaft of the **3**~ ASM in the d and q marks are also shown in Figure 13 and take effect from time t=1s as illustrated below.

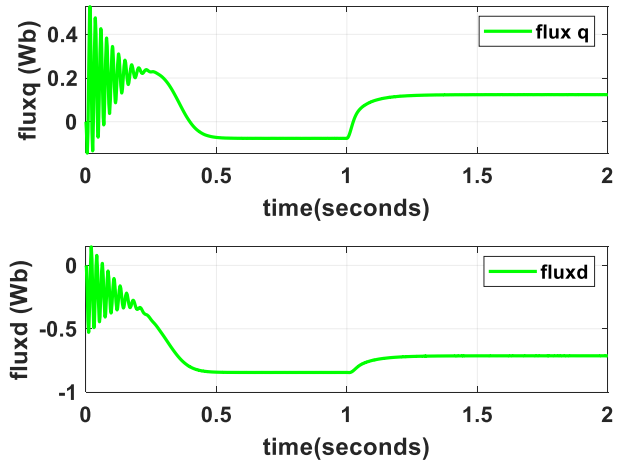

Figure 13: SDCM_V/f 3~ ASM stator flux on load

3.2.2.5. Harmonic Spectrum of Stator Currents

The harmonic spectrum of the on-load stator currents obtained by Fast Fourier Transform between times 1.6 and 1.65 is shown in Figure 14. For a frequency of 50 Hz, it shows a fundamental with an amplitude of approximately 6.5 A. It also has an insignificant overall harmonic distortion of 1.2%.

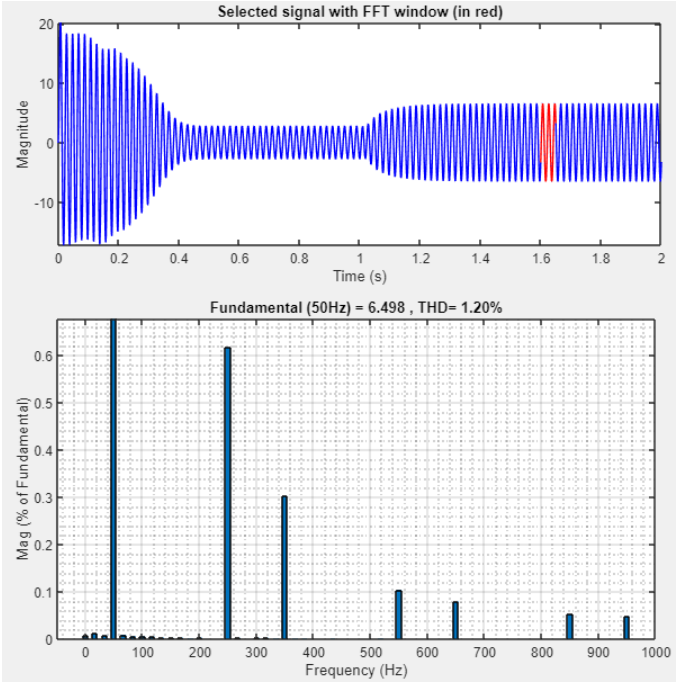

Figure 14: Harmonic spectrum of 3~ ASM currents on load

4. CONCLUSION

In this study, the dynamic model of the three-phase asynchronous motor with cage, as well as the corresponding transformations, were presented. This model was used to investigate the behaviour of the machine using the sinusoidal duty cycle modulation control strategy combined with *V/f* control. Modelling of the MRCS control structure, the inverter and the three-phase asynchronous machine was carried out, followed by simulations in the Matlab-Simulink environment. The results of the open-loop control of the MAS3 were presented and analysed in the previous section. Considering a mechanical load with a resistive torque of 10 Nm, the output speed decreases, while the stator currents increase, adopting a balanced sinusoidal configuration with an exceptionally low harmonic distortion rate of 1.20%. Future work will focus on a closed-loop exploration of this system.

REFERENCES

1. Ekpo, Ekom E., et al. **Winding reconfiguration of 5.5 kW three-phase induction motor for improved performance,** *IEEE PES/IAS PowerAfrica. IEEE*, 2021.
2. K. YAZID. **Commande vectorielle de la machine asynchrone avec prise en compte des variations de la constante de temps rotorique**, *Thèse de Magister, U.S.T.H.B d'Alger, Algérie*, Juin 1996.
3. Ghulam Akbar, Mahnoor Mughal, Syed Sabir Hussain Shah Bukhair. **MATLAB /Simulink Modelings and Experimental Design of Variable Frequency Drive for Speed Control of Three-Phase Induction Motor,** International *Journal of Recent Technology and Engineering (IJRTE)*, Vol.8, Issue-2, July 2019.

4. Raichurkar, Priya Subhash, and Asif Liyakat Jamadar. ***V/f* speed control of 3 phase induction motor using space vector modulation,** *International Journal of Engineering Research & Technology* (IJERT) 4.5 (2015).
5. Habbi, Hanan Mikhael D, Hussein Jalil Ajeel, and Inaam Ibrahim Ali. Speed **control of induction motor using PI and *V/f* scalar vector controllers**, *International Journal of Computer Applications* ,151.7 (2016): 36-43.
6. Şuşcă, Mircea, et al. **General-purpose model of a three-phase asynchronous machine for simulation**, *IEEE International Conference on Automation, Quality and Testing, Robotics (AQTR).* IEEE, 2018.
7. Dorji, Pema, and Bevek Subba. **DQ Mathematical Modelling and Simulation of Three-Phase Induction Motor for Electrical Fault Analysis**,Iarjset 7.9 (2020): 38-46.
8. G. Sonfack, J. Mbihi, and B. L. Moffo. Optimal **duty-cycle modulation scheme for analog-to-digital conversion systems**, *International Journal of Electronics and communication engineering,World Academic of Science, Engineering and Technology*, Vol. 11,no. 3, pp. 354–360, 2017.
9. B. M. Lonla, J. Mbihi, and L. N. Nneme**, Fpga-based multichannel digital duty-cycle modulation and application to simultaneous generation of analog signals,** *STM Journal of Electronic Design Technology (JoEDT),* Vol. 8, no. 1, pp. 23–35, 2017.
10. J. Mbihi, B. Ndjali, and M. Mbouenda. **Modelling and simulation of a class of duty cycle modulators for industrial instrumentation**, *Iranian Journal of Electrical and Computer Engineering*, Vol.4, N°2, pp. 121-128, 2005.
11. J. Mbihi, F. Ndjali Beng, M. Kom, and L. NnemeNneme.**A novel analog-to-digital conversion technique using nonlinear duty-cycle modulation**, *International Journal of Electronics and Computer Science Engineering*, Vol. 1, Number 3, pp. 818-825, 2012.
12. J. Mbihi, L. Nneme Nneme. **A multi-channel analog-todigital conversion technique using parallel duty-cycle modulation**, *International Journal of Electronics and Computer Science Engineering*, Vol. 1, Number 3, pp. 826-833, 2012.
13. B. MoffoLonla, J. Mbihi, L. Nneme Nneme, and M. Kom. A **novel digital-to-analog Conversion technique using duty-cycle modulation**, *International Journal of Circuits, Systems and Signal Processing*, Issue 1, Vol. 7, pp. 42-49, 2013.
14. B. MoffoLonla, J. Mbihi, L. NnemeNneme, and M. Kom . **A Low Cost and High-Quality Duty-Cycle Modulation Scheme and Applications**, *International Journal of Electrical, Computer, Energetic, Electronic and Communication Engineering* Vol:8, No:3, 2014.
15. L. N. Nneme, B. M. Lonlaand J. Mbihi **Review of a Multipurpose Duty-Cycle Modulation Technology in Electrical and Electronics Engineering,** p. 10.
16. J. Mbihi, L. NnemeNneme **virtual simulation and comparison of sine pulse zidthand sine duty cycle modulation drivers for single phase power inverters**, JEEECCS, Volume 6, Issue 21, pages 31-38,2020.
17. M.J.P.Pesdjock, J.R.M.Pone, D.Tchiotsop, M.R.Douanla, G. Kenne .**Minimization of currents harmonics injected for grid connected photovoltaic system using duty cycle modulation technique**, International Journal of dynamic and control, 31 October 2020.
18. A. O. Biyobo, L. N. Nneme, et J. Mbihi. **A Novel Sine Duty-Cycle Modulation Control Scheme for Photovoltaic Single-Phase Power Inverters**, Vol. 17, p. 9, 2018.
19. P. O. Etouke, L. N. Nneme, J. Mbihi. **An Optimal Control Scheme for a Class of Duty-Cycle Modulation Buck Choppers: Analog Design and Virtual Simulation**, *Journal of Electrical Engineering, Electronics, Control and Computer Science* –JEEECCS, Vol 6, Issue 19, pages 13-20, 2020.
20. Y. P. DangweSounsoumo, Jean Mbihi, Haman-djalo and Joseph Yves Effa. Virtual **Digital Control Scheme for a Duty-Cycle Modulation Boost Converter**, *Journal of Computer Science and Control Systems*, Vol 10, No 2, pp. 22-27, October 2017, Romania.
21. Y. P. DangweSounsoumou, HamanDJALO, Jean Mbihi et J. Y. EFFA**. Modélisation et simulation virtuelle d"un nouveau schéma de réglage de hacheurs Boost à commande rapprochée par modulation en rapport cyclique**, *Journal Afrique Science Côte d'Ivoire*, pp. 176-185, Vol. 13, No. 1, 2017.
22. J. Mbihi, L. Nneme Nneme. **A novel Control Scheme for Buck Power Converters using Duty-Cycle Modulation**, *International Journal of Power Electronics*, Vol. 5, N°3/4, pp 185 - 199, October 2013, Switzerlan.
23. Nguefack Tatou Laurel, Paune Felix, Kenfack W. Gutenberg, Mbihi Jean **A Novel Optical Fiber Transmission System UsingDuty-Cycle Modulation and Application to ECG Signal: Analog Design and Simulation**, *Journal of Electrical Engineering, Electronics, Control and Computer Science* – JEEECCS, Volume 6, Issue 21, pages 39-48, 2020.
24. Otam Steve Ulriche, MoffoLonla Bertrand, GamomNgounou E. R. Christian, Mbihi Jean. **A novel FPGA-Based Multi-Channel Signal Acquisition System Using Parallel Duty-Cycle Modulation and Application to BiologicSignals: Design and Simulation, Journal** *of Electrical Engineering, Electronics, Control and Computer Science* –JEEECCS, Vol 7, Issue 24, pages 13-20, 2021.
25. G.R Tobajio Haoudou, A. Biyobo Obono, Léandre.N. Nneme. **Design and Simulation of a New Topology of Single-Phase Stand-Alone Solar**

Inverters by Sinusoidal Duty Cycle Modulation, *International Journal of Scientific Research and Engineering Development*—IJSRED, Volume 5, Issue 2, pages 154-161, 2022.

26. G.R Tobajio Haoudou, A. Biyobo Obono, Léandre.N. Nneme, Jean MBIHI**. Design and Simulation of Grid-Connected Photovoltaic Single-Phase Inverters» International Journal of Emerging Trends in Engineering Research,** IJETER, Volume 10. No.10, October 2022.